World Journal of Applied Chemistry
2026, Vol. 11, No. 3, pp. 86–100
https://doi.org/10.11648/j.wjac.20261103.13

Research Article

Adsorptive Removal of Pb(II), Ni(II), and Co(II) from Simulated Wastewater Using Delonix Regia Seed: Equilibrium and Kinetic Studies

Oyewole Toyib Seun[1], Osundiya Medinat Olubunmi[1], Agumadu Emmanuel Chukwuma[2], Ogunbamowo Haminat Temidayo[1], Salawu Ismael Eyue[1], Idowu Owoyemi Fatai[1], Badejo Olayemi Aderanti[3], Olowu Rasaq Adewale[1,*]

[1]Department of Chemistry, Lagos State University, Ojo, Nigeria

[2]Quality Control Department, National Agency for Food and Drug Administration and Control, Lagos, Nigeria

[3]Department of Chemistry, Lagos State University of Education, Ijanikin, Nigeria

Abstract

The development of low-cost biosorbents from agricultural biomass offers a sustainable approach for the remediation of heavy metal-contaminated wastewater. In this study, Delonix regia seed (DRS) was evaluated as a natural biosorbent for the removal of Pb(II), Ni(II), and Co(II) ions from simulated wastewater. The adsorbent was characterized using X-ray diffraction (XRD), scanning electron microscopy (SEM), and Fourier-transform infrared spectroscopy (FTIR), revealing an amorphous surface enriched with hydroxyl and carbonyl functional groups that participate in metal ion binding. Batch adsorption experiments were conducted to investigate the effects of solution pH, adsorbent dosage, initial metal ion concentration, contact time, and temperature. Maximum removal efficiencies exceeding 90% were achieved under optimized conditions. Equilibrium data were best described by the Langmuir isotherm, with maximum monolayer adsorption capacities of 62.57 mg g^{-1} for Pb(II), 59.26 mg g^{-1} for Co(II), and 73.59 mg g^{-1} for Ni(II), indicating favorable monolayer adsorption on a homogeneous surface. Kinetic analysis showed that the adsorption process followed the pseudo-second-order model, suggesting that chemisorption is the dominant rate-controlling mechanism. The combined characterization and adsorption results demonstrate that Delonix regia seed is an abundant, inexpensive, and environmentally sustainable biosorbent with considerable potential for heavy metal removal in wastewater treatment applications.

Keywords

Delonix Regia, Biosorption, Pb(II), Ni(II), Co(II), Adsorption Isotherm, Adsorption Kinetics

*Correspondence: Olowu Rasaq Adewale (rasaq.olowu@lasu.edu.ng)

Received: 30 August 2026; **Accepted:** 9 September 2026; **Published:** 24 September 2026

1. Introduction

Heavy metal contamination of aquatic environments has become one of the most persistent environmental challenges, driven by rapid industrialization, urbanization, mining, electroplating, battery manufacturing, and metallurgical operations [2]. Unlike organic pollutants, heavy metals are non-biodegradable and can accumulate in living organisms, posing serious ecological and public health risks through bioaccumulation and biomagnification. Lead (Pb), nickel (Ni), and cobalt (Co) are among the most hazardous metallic contaminants because prolonged exposure has been associated with neurological disorders, kidney dysfunction, carcinogenicity, and impairment of aquatic ecosystems. [3, 19].

Conventional technologies for heavy metal removal, including chemical precipitation, ion exchange, membrane filtration, coagulation-flocculation, and electrochemical treatment, have demonstrated high removal efficiencies [4]. However, these methods often incur high operational costs, generate excessive sludge, cause membrane fouling, and require complex maintenance, limiting their widespread application, particularly in developing countries [5]. Consequently, adsorption has emerged as one of the most attractive alternatives owing to its operational simplicity, high efficiency, economic feasibility, and adaptability for treating dilute metal-containing wastewater [6].

In recent years, considerable attention has been directed toward the development of biomass-derived adsorbents from agricultural residues because they are renewable, biodegradable, inexpensive, and rich in oxygen-containing functional groups capable of binding metal ions through ion exchange, electrostatic attraction, surface complexation, and chelation mechanisms [7-9]. Numerous agricultural materials, including rice husk, banana peel, coconut shell, maize cob, cassava peel, and fruit seeds, have been investigated as sustainable biosorbents with encouraging adsorption performances [18].

Delonix regia (Royal Poinciana) is a widely distributed tropical tree whose seeds constitute an abundant agricultural by-product that is frequently discarded as waste [10]. The lignocellulosic matrix of the seed contains cellulose, hemicellulose, lignin, proteins, and phenolic constituents bearing hydroxyl, carbonyl, and carboxyl functional groups that can effectively coordinate divalent metal ions [11-13]. Although previous studies have explored Delonix regia pods and biochar derived from its seeds for selected metal removal, investigations involving the raw, unmodified seed for the simultaneous adsorption of Pb(II), Ni(II), and Co(II) remain limited [34]. Furthermore, comparative adsorption behaviour among these three environmentally significant metal ions has not been comprehensively evaluated using equilibrium and kinetic modelling on untreated Delonix regia seed [1]. Understanding the differences in adsorption affinity is essential for designing economical biosorbents suitable for multi-metal wastewater treatment systems [14, 15].

Therefore, this study investigates the adsorption performance of raw Delonix regia seed for the removal of Pb(II), Ni(II), and Co(II) ions from simulated wastewater. The biosorbent was characterized using XRD, SEM, and FTIR techniques, while the influences of pH, adsorbent dosage, initial concentration, contact time, and temperature were systematically evaluated. In addition, Langmuir, Freundlich, and Temkin isotherms together with pseudo-first-order and pseudo-second-order kinetic models were employed to elucidate the adsorption mechanism and identify the governing adsorption behaviour.

2. Materials and Methods

2.1. Preparation of *Delonix regia* Seed Adsorbent

Delonix regia seeds were collected from the Lagos State University, Ojo Campus, Lagos State, Nigeria (6.47 °N, 3.2 °E). The collected seeds were cut into pieces of approximately 1-2 cm and thoroughly washed with deionized water to remove adhering surface contaminants. The washed seeds were oven-dried at 80 ℃ for 24 h. The dried material was subsequently crushed to reduce the particle size and soaked in deionized water for 6 h to remove water-soluble pigments. After soaking, the material was further dried at 80 ℃ for 6 h.

The dried seeds were then subjected to particle-size reduction using a crushing machine and separated using a vibrating sieve. The sieve was mechanically oscillated for 15 min, and the mass of material retained on each sieve was determined by weighing the sieves before and after separation. The particle sizes used in the adsorption experiments ranged from 0.25 to 5 mm. The prepared *Delonix regia* seed (DRS) was used in its natural form without chemical or thermal modification.

2.2. Reagents and Preparation of Metal Ion Solutions

All chemicals used in this study were of analytical grade and were used without further purification. Stock solutions of Pb(II), Ni(II), and Co(II), each at a concentration of 1000 mg L^{-1}, were prepared separately using analytical-grade $Pb(NO_3)_2$, $NiCl_2$ $6H_2O$, and $CoCl_2$ $6H_2O$, respectively. Briefly, 1.599 g of $Pb(NO_3)_2$, 4.050 g of $NiCl_2$ $6H_2O$, and 4.038 g of $CoCl_2$ $6H_2O$ were accurately weighed and separately dissolved in deionized water. Each solution was transferred into a 1 L volumetric flask and made up to the mark with deionized water to obtain the respective 1000 mg L^{-1} stock solutions. The required working concentrations were subsequently prepared by appropriate dilution of the stock solutions with deionized water.

2.3. Characterization of the Adsorbent

The structural characteristics of the raw *Delonix regia* seed were characterized using X-ray diffraction (XRD; Bruker D8 Advance, Bruker AXS, Germany). The surface morphology of the adsorbent before and after metal-ion adsorption was examined using scanning electron microscopy (SEM; JEOL JSM-IT100, JEOL Ltd., Japan). Fourier-transform infrared (FTIR) spectroscopy was performed using an FTIR spectrometer (Bruker Tensor 27, Bruker Optics, Germany) to identify the functional groups present on the adsorbent surface and evaluate their potential roles in metal-ion adsorption.

2.4. Batch Adsorption Experiments

Batch adsorption experiments were conducted to investigate the removal of Pb(II), Ni(II), and Co(II) from aqueous solutions. Unless otherwise stated, 0.6 g of powdered DRS was transferred into a clean, dry 100 mL Erlenmeyer flask, followed by the addition of 50 mL of the corresponding metal-ion solution at an initial concentration of 400 mg L^{-1} [17, 18]. The mixtures were agitated at 100 rpm for 2 h using a mechanical shaker to allow the adsorption system to approach equilibrium. After the specified contact period, the suspensions were filtered, and the residual metal-ion concentrations in the filtrates were determined using atomic absorption spectrophotometry (AAS; Thermo Scientific, Waltham, MA, USA). The pH of the solutions was adjusted to the desired value using 0.1 M HCl or 0.1 M NaOH before the addition of the adsorbent.

2.4.1. Effect of Solution pH

The effect of solution pH on the adsorption of Pb(II), Ni(II), and Co(II) onto DRS was investigated over the pH range of 2-10. The desired pH was adjusted using 0.1 M HCl or 0.1 M NaOH before the addition of the adsorbent. All other experimental conditions were maintained constant. After the specified contact period, the adsorbent was separated from the solution, and the residual metal-ion concentration was determined by AAS.

2.4.2. Effect of Adsorbent Dosage

The effect of adsorbent dosage was investigated by varying the mass of DRS from 0.2 to 1.0 g while maintaining the solution volume, initial metal-ion concentration, agitation speed, and contact time constant. The resulting residual metal-ion concentrations were determined using AAS to evaluate the influence of adsorbent dosage on removal efficiency.

2.4.3. Effect of Initial Metal-Ion Concentration

The influence of initial metal-ion concentration on adsorption was investigated by varying the concentration of Pb(II), Ni(II), and Co(II) solutions from 100 to 500 mg L^{-1} while maintaining the other experimental conditions constant. After equilibration, the suspensions were filtered, and the residual metal-ion concentrations were determined by AAS.

2.4.4. Effect of Contact Time

The effect of contact time on the adsorption of Pb(II), Ni(II), and Co(II) was investigated at an initial metal-ion concentration of 400 mg L^{-1}. Contact times ranging from 20 to 100 min were examined while maintaining the adsorbent dosage, solution volume, agitation speed, and other experimental conditions constant. At each specified time interval, the suspension was separated by filtration and the residual metal-ion concentration was determined using AAS.

2.4.5. Effect of Temperature

The influence of temperature on the adsorption process was investigated over the temperature range of 27-67 ℃ using DRS and metal-ion solutions with an initial concentration of 400 mg L^{-1}. The experiments were conducted under controlled conditions while maintaining the adsorbent dosage, solution volume, agitation speed, and contact conditions constant. Following equilibration, the residual concentrations of Pb(II), Ni(II), and Co(II) were determined by AAS.

The adsorption capacity (Q_e) and the percentage removal efficiency (%R) were calculated using Equations (1) and (2)

$$Q_e = \frac{(C_o - C_e)}{m} \times V \quad (1)$$

$$\%R = \frac{C_o - C_e}{C_o} \times 100 \quad (2)$$

where: C_0 = initial concentration (mg L^{-1}), C_e = equilibrium concentration (mg L^{-1}), V = volume of solution (L), and m = mass of adsorbent (g)

2.5. Adsorption Isotherms Studies

Langmuir, Freundlich, and Temkin models are widely recognized as the most frequently utilized isotherm models for activated carbon in water and wastewater treatment [21]. Thus, this study applied these models to the adsorption isotherm analysis. The quantity of metallic ions adsorbed on the various quaternary adsorbents (Q_t) was calculated using Equation (1) as shown below:

$$Q_t = \frac{(C_o - C_t)}{m} \times V \quad (4)$$

In Equation (4), the volume of adsorbate (V) is expressed in (L), while the mass of adsorbent (m) is given in (g). The initial concentration of metallic ions in the adsorbate (C_0) is stated in (mg L^{-1}), and the concentration of metallic ions remaining in the adsorbate at a specific time (C_t) is also given in (mg L^{-1}). The concentrations of adsorbate that do not change over time in various adsorption processes are recorded as equilibrium concentrations (C_e). To determine the

adsorption isotherm governing the removal of metallic ions (such as Pb^{2+}, Ni^{2+}, and Co^{2+}) from the adsorbate by the adsorbent, graphs of log qt against log C_e (for the Freundlich model) are plotted. $\frac{1}{qt}$ against $\frac{1}{Ce}$ (for the Langmuir model), and Q_e against ln C_e (for the Temkin model). Thereafter, the best-fitted equations from the plots were compared to the linearized forms of the Langmuir, Freundlich, and Temkin isotherm models, which were used to determine the adsorption capacities. The model that provided higher values of the coefficient of determination (R^2) was considered the adsorption isotherm governing the adsorption process. The linearized form of the Freundlich isotherm model is expressed in Equation (5) as follows:

$$Log\ \ Q_t = \frac{1}{n}\log C_e + Log\ \ K_f \tag{5}$$

where: Q_t is the amount of ions adsorbed on the adsorbent (mg g^{-1}), C_e is the equilibrium concentration (mg L^{-1}), K_F is the Freundlich constant, which indicates the adsorption capacity of the adsorbent (mg g^{-1}), and n is the Freundlich constant, which indicates adsorption intensity (g L^{-1}). On the other hand, the linearized form of the Langmuir isotherm model is given in Equation (6) below:

$$\frac{Ce}{Qe} = \frac{1}{Qm\ K}\ \ C_e\ \ + \frac{1}{Qm} \tag{6}$$

In Equation (6), Qe is the amount of ions adsorbed on the adsorbent (mg g^{-1}), C_e is the equilibrium concentration (mg L^{-1}), Qm is the monolayer adsorption capacity at equilibrium (mg g^{-1}), and K is the Langmuir equilibrium constant (L mg^{-1}). Lastly, the linearized form of the Temkin isotherm model is given in Equation (7) below:

$$Q_e = \frac{RT}{B_t}\ln A_t + \frac{RT}{B_t}\ln C_e \tag{7}$$

The Temkin isotherm model describes B_t as a constant that is related to the heat of adsorption and A_t as the equilibrium binding constant (L g^{-1}).

The essential features of the isotherm were expressed in terms of a dimensionless constant, the separation factor (R_L), defined by the relationship:

$$R_L = \frac{1}{1+KL\ \ Co} \tag{8}$$

where C_o is the initial concentration (mg/L), K_L is the Langmuir equilibrium constant (L/mg).

The value of the separation factor (R_L) provides important information about the nature of adsorption. The value of (R_L) indicates the type of Langmuir isotherm to be irreversible (R_L = 0), favourable (0<R_L<1), linear (R_L =1), or unfavourable (R_L >1). Apparently, when K_L>1, sorption is favorable [40].

2.6. Adsorption Kinetics Studies

The amount of ions adsorbed at equilibrium (mg/g) at different contact times t was determined and recorded as Qe through Equation (9) stated below:

$$Q_e = \frac{(Co-Ce)}{m} \times V \tag{9}$$

All symbols in Equation (9) remain the same as previously explained. Graphs were plotted based on the linearized forms of pseudo-first-order and 2nd-order kinetics. The rate constants of adsorption were determined by comparing the equation of the best-fitted plots with the linearized forms of pseudo-first-order and 2nd order kinetics given in Equations (10) and (11), respectively.

$$\text{Log } (Q_e\text{-}Q_t) = \text{Log } (Q_e) - (\frac{K_t}{2.303})t \tag{10}$$

$$\frac{t}{Q_t} = \frac{1}{K_2 Q_e{}^2} + \frac{1}{Q_e}t \tag{11}$$

Equations (10) and (11) indicate that K_1 and K_2 are the rate constants for pseudo-first-order and 2nd order adsorption, respectively, with units of min^{-1} and g mg^{-1} min^{-1}. The other symbols in the equations are the same as those previously explained. The order of the kinetics governing the adsorption process was determined by examining the coefficient of determination (R^2) values associated with the best-fitted plots for the equation.

3. Results and Discussion

3.1. Characterization of *Delonix Regia* Seed

3.1.1. X-ray Diffraction Analysis

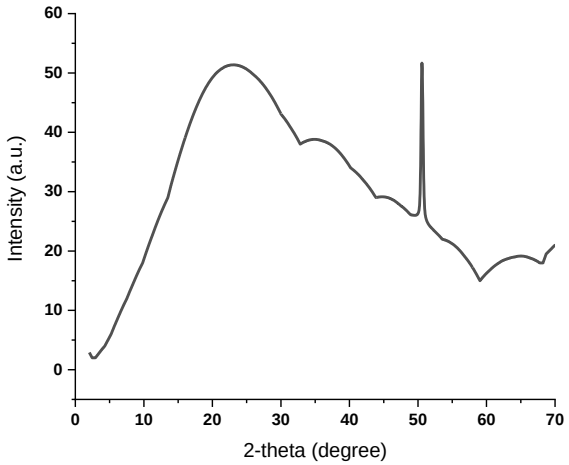

Figure 1. *XRD plot of Delonix regia seed.*

The structural characteristics of the raw *Delonix regia* seed were investigated using X-ray diffraction (XRD), and the resulting diffractogram is presented in Figure 1. The pattern is characterized by a broad, diffuse diffraction profile rather than distinct, sharp reflections, indicating that the biosorbent is predominantly amorphous [22]. This structural characteristic is consistent with the complex organic composition of plant biomass, which contains cellulose, hemicellulose, lignin, proteins, and other organic constituents with limited long-range molecular ordering [23-25]. The predominantly amorphous structure may provide a relatively disordered surface containing accessible functional groups that can participate in the adsorption of metal ions [26, 27].

3.1.2. Scanning Electron Microscope (SEM) Analysis

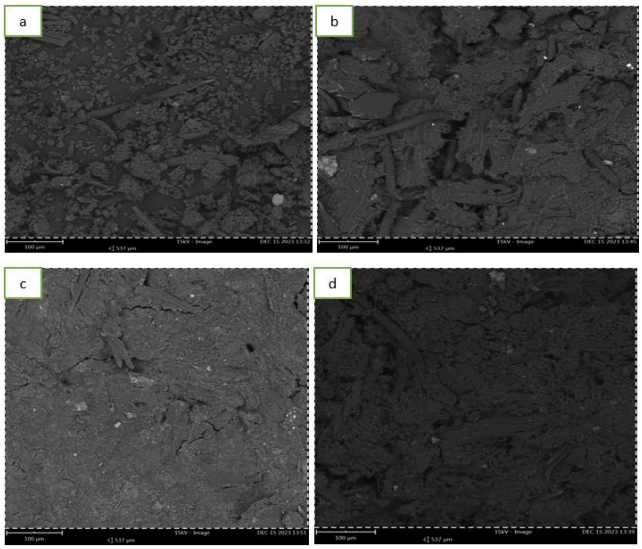

Figure 2. *SEM images of Delonix regia seed residue (a): before adsorption; (b, c, and d) post-adsorption of Pb^{2+}, Co^{2+}, and Ni2+, respectively.*

The surface morphology of the raw and metal-loaded *Delonix regia* seed was examined using scanning electron microscopy (SEM), as shown in Figure 2. The raw adsorbent exhibited an irregular and heterogeneous surface characterized by visible pits, depressions, ridges, and grooves (Figure 2a). These surface features provide accessible regions that may facilitate the interaction of dissolved metal ions with the adsorbent. Following adsorption, noticeable changes in surface morphology were observed for the Pb(II)-, Co(II)-, and Ni(II)-loaded adsorbents (Figure 2b-d). The post-adsorption surfaces appeared comparatively rougher, with partial coverage of the original surface features [30]. These changes may be associated with the deposition and interaction of metal ions with active sites on the biomass surface. The observed morphological modifications following metal-ion exposure provide qualitative evidence of interaction between the adsorbent surface and the investigated metal ions.

3.1.3. Fourier Transform Infrared Spectroscopy (FTIR) Analysis

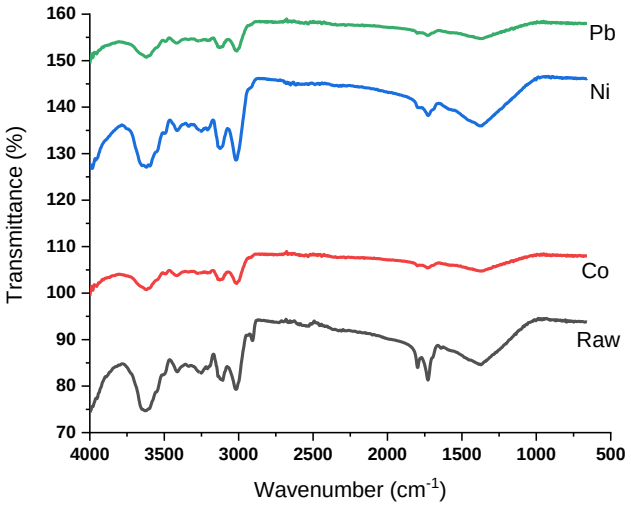

Figure 3. *FTIR Results of raw Delonix regia seeds before and after adsorption of Pb^{2+}, Ni^{2+}, and Co^{2+}.*

The FTIR spectra of raw *Delonix regia* seeds and the adsorbent after Pb(II), Co(II), and Ni(II) adsorption are presented in Figure 3. The spectrum of the raw adsorbent exhibited a prominent band at 3597.33 cm^{-1}, which can be attributed to O-H stretching vibrations associated with hydroxyl-containing constituents of the biomass. Following metal-ion adsorption, the corresponding bands shifted slightly to 3582.43 cm^{-1} for Co(II), 3589.88 cm^{-1} for Ni(II), and 3593.30 cm^{-1} for Pb(II), accompanied by changes in band intensity [28]. These shifts suggest that hydroxyl-containing functional groups may interact with metal ions. Additional bands were observed around 3000 cm^{-1}, which may be associated with C-H stretching vibrations of organic constituents of the biomass. The band at 1713.38 cm^{-1} in the raw adsorbent is attributed to C=O stretching vibrations. Changes in the intensity and position of this band following adsorption, particularly for Co(II) and Pb(II), suggest the possible involvement of carbonyl-containing functional groups in metal-ion binding [11]. The observed spectral changes, together with the morphological changes identified by SEM, provide evidence that surface functional groups of *Delonix regia* seed participate in the adsorption of Pb(II), Co(II), and Ni(II).

3.2. Effect of Operational Parameters on Adsorption Performance

3.2.1. Effect of pH

Solution pH is an important parameter governing metal-ion adsorption because it affects the protonation state and surface

charge of the adsorbent as well as the aqueous speciation of metal ions. As shown in Figure 4, the percentage removal of Pb(II), Co(II), and Ni(II) increased progressively with increasing solution pH. At lower pH values, the relatively low adsorption efficiency can be attributed to the protonation of surface functional groups, which reduces the availability of negatively charged sites for interaction with the positively charged metal ions [31]. In addition, the high concentration of H^+ ions creates competition between protons and metal ions for available adsorption sites. As the pH increases, progressive deprotonation of surface functional groups can increase the availability of binding sites and enhance metal-ion uptake. The improved removal at higher pH values may therefore be associated with increased availability of surface functional groups for metal binding [32]. However, at sufficiently high pH, the formation of metal hydroxide species may also contribute to the observed decrease in dissolved metal concentration. Therefore, the enhanced removal observed under alkaline conditions should be interpreted as the combined effect of adsorption and possible changes in metal-ion speciation rather than being attributed exclusively to surface adsorption.

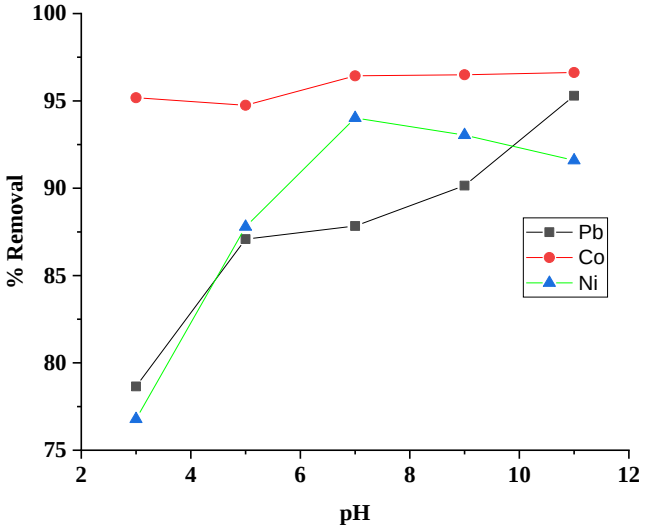

Figure 4. *The graph of% removal of Pb^{2+}, Co^{2+} and Ni^{2+} against pH.*

3.2.2. Effect of Adsorbent Dose

The effect of *Delonix regia* seed dosage on the removal of Pb(II), Co(II), and Ni(II) is presented in Figure 5. Increasing the adsorbent dosage from 0.2 to 1.0 g resulted in a progressive increase in metal-ion removal. At the highest dosage investigated (1.0 g), removal efficiencies of 89.3%, 97.94%, and 92.4% were obtained for Pb(II), Co(II), and Ni(II), respectively. The increase in removal efficiency with increasing adsorbent dosage can be attributed primarily to the greater availability of surface-active sites and the increased total surface area available for metal-ion interaction [29]. Increasing the mass of biosorbent also provides a greater number of binding sites relative to the amount of metal ions present in solution, thereby enhancing the overall percentage removal. Because the present experiment was limited to a maximum dosage of 1.0 g, this value is regarded as the highest dosage investigated rather than a definitive optimum dosage. Further experiments at higher dosages would be required to establish whether an adsorption plateau or optimum dosage exists.

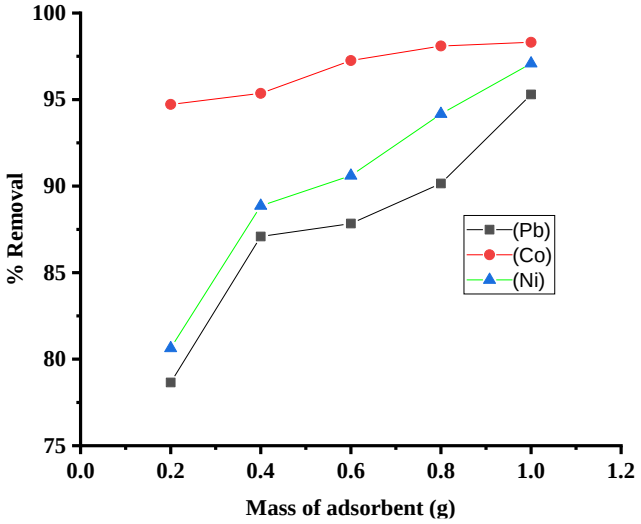

Figure 5. *The graph of% removal of Pb^{2+}, Co^{2+} and Ni^{2+} against adsorbent dose.*

3.2.3. Effect of Concentration

The effect of initial metal-ion concentration on Pb(II), Co(II), and Ni(II) removal is presented in Figure 6. Increasing the initial metal-ion concentration from 100 to 500 mg L^{-1} resulted in a slight decrease in percentage removal for the investigated metal ions, whereas the corresponding adsorption capacity increased. At lower initial concentrations, a relatively large proportion of the available adsorption sites remained accessible compared with the number of metal ions present in solution, resulting in higher percentage removal. As the initial concentration increased, the available adsorption sites became progressively occupied, and competition among metal ions for the remaining active sites increased [23]. This resulted in a reduction in the fraction of metal ions removed from solution.

In contrast, the increase in adsorption capacity with increasing initial concentration reflects the greater concentration gradient between the aqueous phase and the adsorbent surface, which provides a stronger driving force for mass transfer and promotes greater uptake per unit mass of adsorbent. The observed behaviour demonstrates that initial concentration influences both the percentage removal and the amount of metal ions retained by the biosorbent.

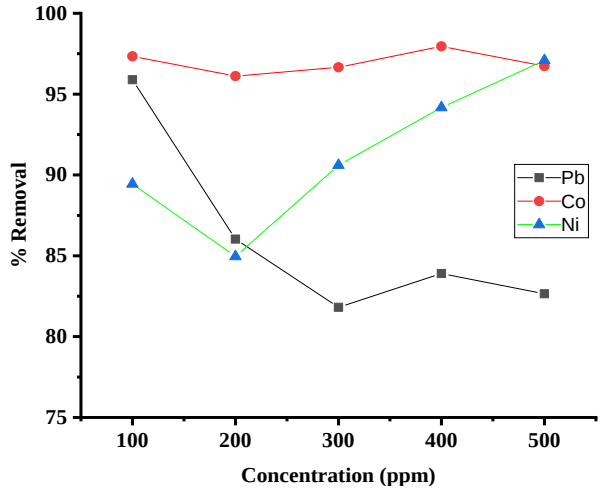

Figure 6. *The graph of% removal of Pb^{2+}, Co^{2+} and Ni^{2+} against concentration.*

3.2.4. Effect of Temperature

The influence of temperature on the adsorption of Pb(II), Co(II), and Ni(II) onto *Delonix regia* seed is presented in Figure 7. An increase in temperature from 27 to 67 ℃ resulted in enhanced removal efficiencies for the three metal ions. The increase in adsorption with temperature suggests that elevated temperature favours the interaction between the dissolved metal ions and the active sites of the biosorbent. Increasing temperature may enhance the mobility of metal ions in solution and facilitate their diffusion toward accessible adsorption sites [30]. It may also promote interactions between the metal ions and functional groups present on the biomass surface. The observed temperature dependence suggests that the adsorption process is favoured at elevated temperatures. However, the thermodynamic parameters, particularly the standard enthalpy change (ΔH°), provide a more direct basis for determining whether the overall adsorption process is endothermic or exothermic [32].

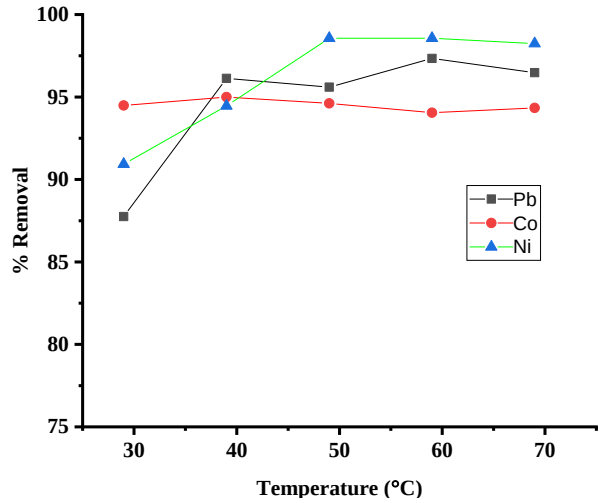

Figure 7. *The graph of% removal of Pb^{2+}, Co^{2+} and Ni^{2+} against temperature.*

3.2.5. Effect of Contact Time

The influence of contact time on the adsorption of Pb(II), Co(II), and Ni(II) onto *Delonix regia* seed is presented in Figure 8. A rapid increase in metal-ion removal was observed during the initial stage of the adsorption process, particularly within the first 20-60 min, followed by a more gradual increase as the contact time increased. The rapid initial uptake can be attributed to the abundance of readily accessible adsorption sites on the fresh biosorbent surface [41]. As adsorption progressed, an increasing proportion of these sites became occupied, resulting in a gradual reduction in the rate of metal-ion uptake. In addition, diffusion of metal ions toward less accessible regions of the biomass may contribute to the slower adsorption observed at longer contact times [14]. The adsorption approached a near-steady state at approximately 100 min under the conditions investigated. This contact time was therefore considered appropriate for the subsequent equilibrium studies.

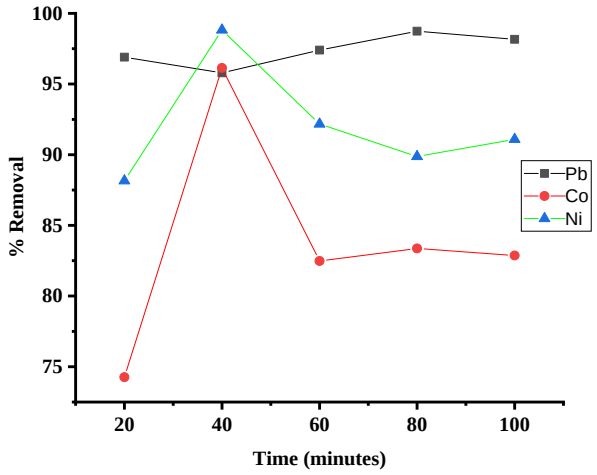

Figure 8. *The graph of% removal of Pb^{2+}, Co^{2+} and Ni^{2+} against time.*

3.3. Equilibrium Adsorption Isotherms

The equilibrium adsorption behaviour of Pb(II), Co(II), and Ni(II) onto *Delonix regia* seed was evaluated using the Langmuir, Freundlich, and Temkin isotherm models. The corresponding linearized plots are presented in Figures 9-11, while the calculated isotherm parameters are summarized in Table 1. The Langmuir model provided the highest coefficient of determination for Pb(II) and Co(II), with R^2 values of 0.989 and 0.996, respectively. For Ni(II), the Langmuir model gave an R^2 value of 0.947, while the Temkin model produced a comparable value of 0.942. Thus, the equilibrium data for Pb(II) and Co(II) were better described by the Langmuir model, whereas both the Langmuir and Temkin models provided comparable descriptions of Ni(II) adsorption. The Langmuir maximum adsorption capacities were 62.57 mg g^{-1} for Pb(II),

59.26 mg g^{-1} for Co(II), and 73.59 mg g^{-1} for Ni(II). The resulting capacity followed the order Ni(II) > Pb(II) > Co(II), indicating a comparatively greater adsorption capacity toward Ni(II) under the investigated conditions. Differences in adsorption capacity among the metal ions may arise from variations in their hydration characteristics, ionic properties, and interactions with the functional groups present on the biomass surface [36]. The calculated Langmuir separation factors (R_L) were 0.046, 0.098, and 0.096 for Pb(II), Co(II), and Ni(II), respectively. Since all values fall within the range $0 < R_L < 1$, the adsorption process can be considered favourable under the investigated conditions [20]. The Freundlich model produced lower correlation coefficients for all three metal ions, with R^2 values ranging from 0.831 to 0.887. This indicates that the Freundlich model provided a comparatively poorer description of the equilibrium data. The Temkin model gave moderate fits, with R^2 values of 0.926, 0.943, and 0.942 for Pb(II), Co(II), and Ni(II), respectively [1]. The isotherm results indicate that monolayer-type adsorption provides a useful description of Pb(II) and Co(II) adsorption onto *Delonix regia* seeds, while the comparable Langmuir and Temkin fits for Ni(II) suggest that both surface coverage and adsorbent-adsorbate interactions may contribute to its equilibrium behavior [37].

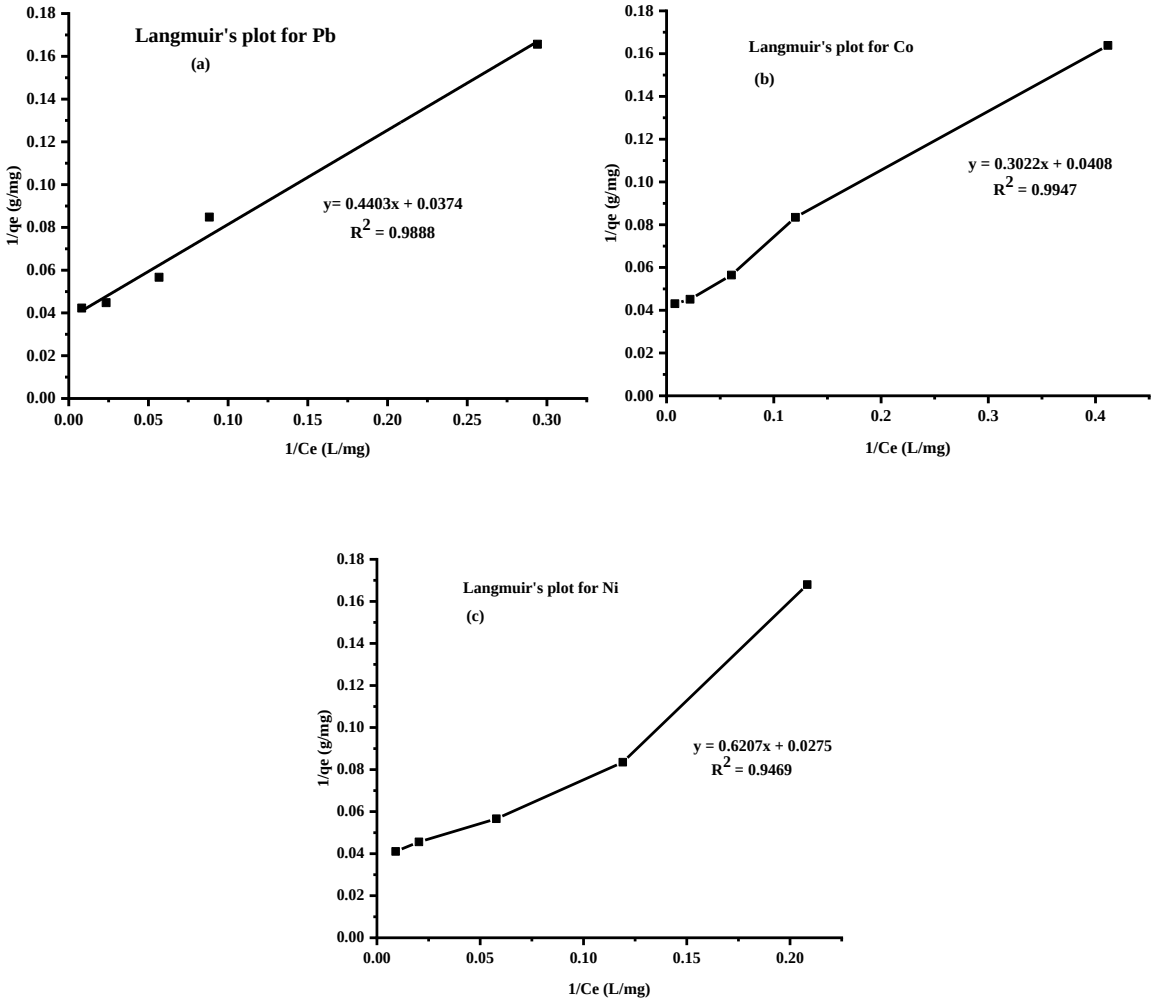

Figure 9. *Langmuir linear plot for adsorption of (a) Pb^{2+}, (b) Co^{2+}, and (c) Ni^{2+} onto Delonix Regia seed.*

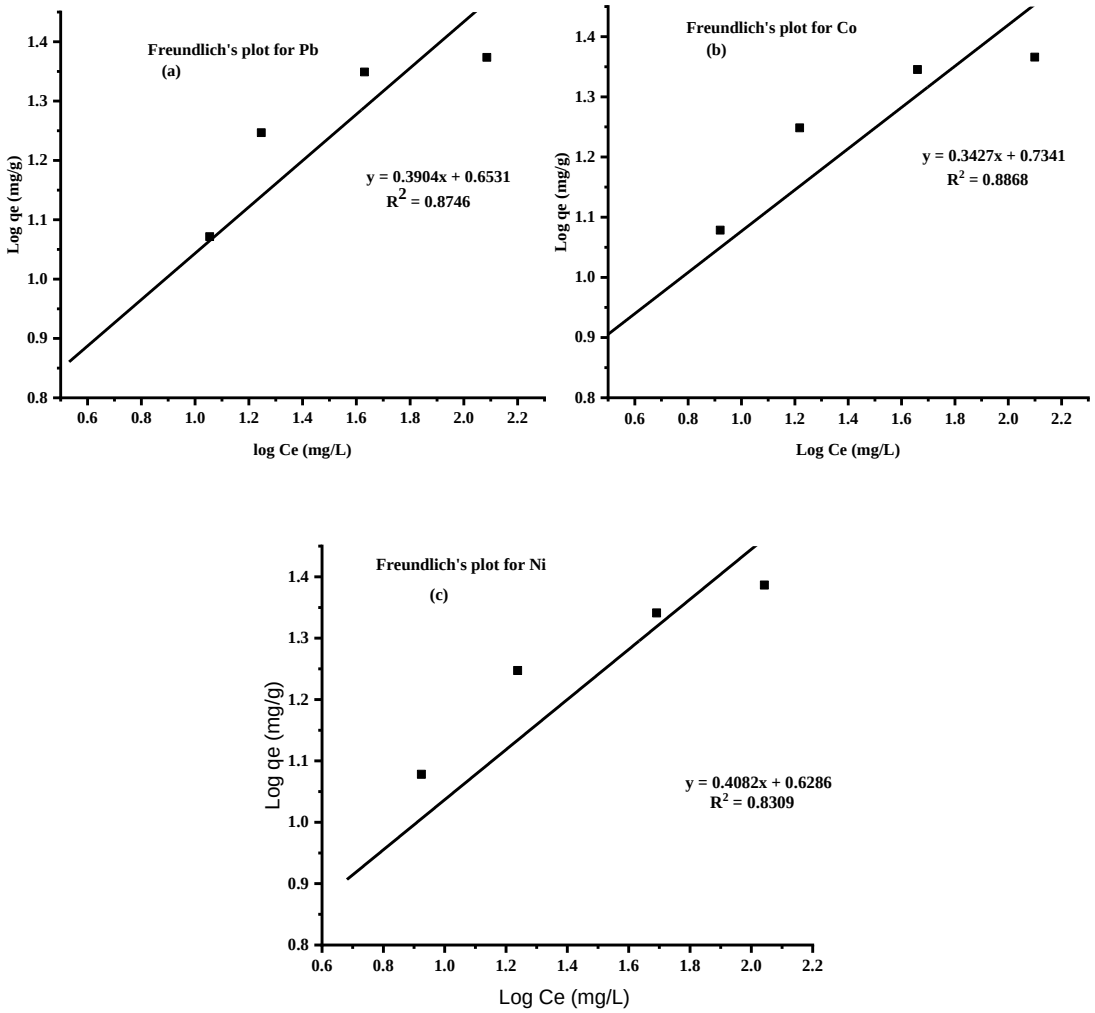

Figure 10. *Freundlich linear plot for adsorption of (a) Pb^{2+}, (b) Co^{2+}, and (c) Ni^{2+} onto Delonix Regia seed.*

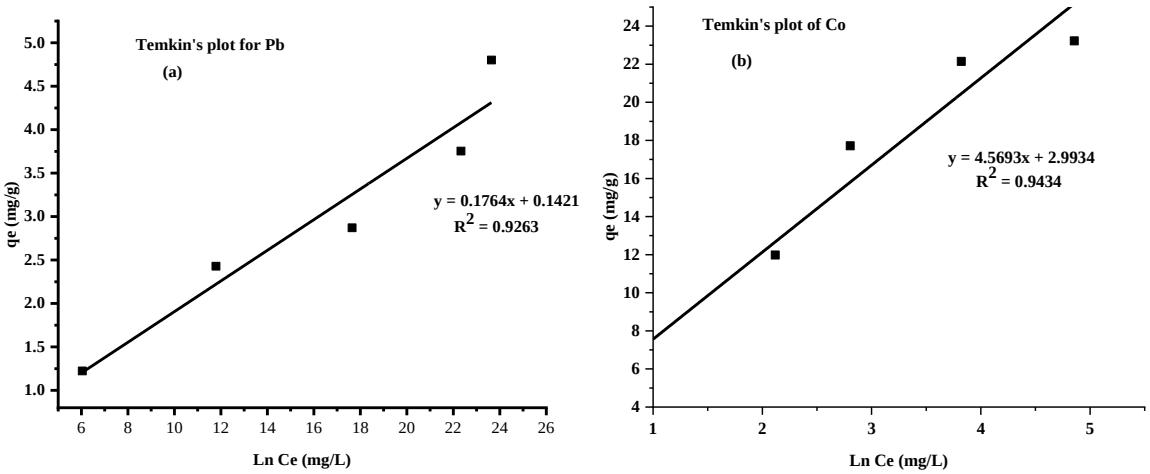

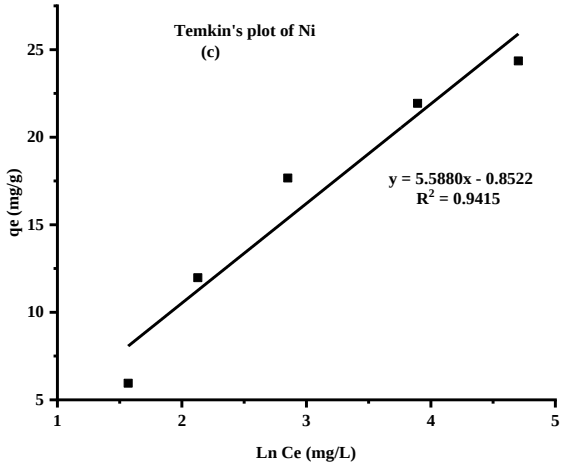

Figure 11. *Temkin linear plot for adsorption of (a) Pb^{2+}, (b) Co^{2+}, and (c) Ni^{2+} onto Delonix Regia seed.*

Table 1. *Parameters for various isotherm models of Pb^{2+}, Co^{2+}, and Ni^{2+} ions onto DRS.*

Isotherms	Pb^{2+}	Co^{2+}	Ni^{2+}
Langmuir			
Q_{max} (mg g^{-1})	62.57	59.26	73.59
K_L	1.191	0.847	0.153
R_L (L mg^{-1})	0.046	0.098	0.096
R^2	0.989	0.996	0.947
Freundlich			
n	3.827	2.139	4.362
K_F (mg g^{-1})	1.543	1.034	1.374
R^2	0.875	0.887	0.831
Temkin			
B_T (J mol^{-1})	1.681	2.697	3.522
K_T (L g^{-1})	0.823	0.744	0.935
R^2	0.926	0.943	0.942

3.4. Adsorption Kinetics Studies

The adsorption kinetics of Pb(II), Co(II), and Ni(II) onto *Delonix regia* seeds were evaluated using pseudo-first-order and pseudo-second-order kinetic models. The corresponding linear plots are presented in Figures 12 and 13, and the calculated kinetic parameters are summarized in Table 2. The pseudo-first-order model gave correlation coefficients of 0.8778, 0.8834, and 0.8694 for Pb(II), Co(II), and Ni(II), respectively. These relatively moderate correlation coefficients indicate that the model did not adequately describe the experimental adsorption behaviour. In addition, the calculated equilibrium adsorption capacities differed from the experimentally observed values [16]. The pseudo-second-order model produced substantially higher correlation coefficients for Pb(II) and Ni(II), with R^2 values of 0.9998 and 0.9989, respectively. For Co(II), the pseudo-second-order model also provided a better fit than the pseudo-first-order model, although the corresponding R^2 value of 0.8834 indicates a comparatively weaker fit. The calculated equilibrium capacities from the pseudo-second-order model were also closer to the experimental values, particularly for Pb(II) and Ni(II). The better performance of the pseudo-second-order model suggests that adsorption involving the available surface binding sites plays an important role in the uptake of the metal ions [38]. However, pseudo-second-order kinetics alone cannot be considered definitive evidence of chemisorption because the model is an empirical kinetic expression and may provide a good fit under different adsorption mechanisms [39]. The differences in kinetic behaviour among Pb(II), Co(II), and Ni(II) may be related to differences in their aqueous properties and interactions with the functional groups present on the *Delonix regia* seed surface [35]. Overall, the kinetic results demonstrate that the pseudo-second-order model provides a better mathematical description of the adsorption data than the pseudo-first-order model, particularly for Pb(II) and Ni(II) [33, 34].

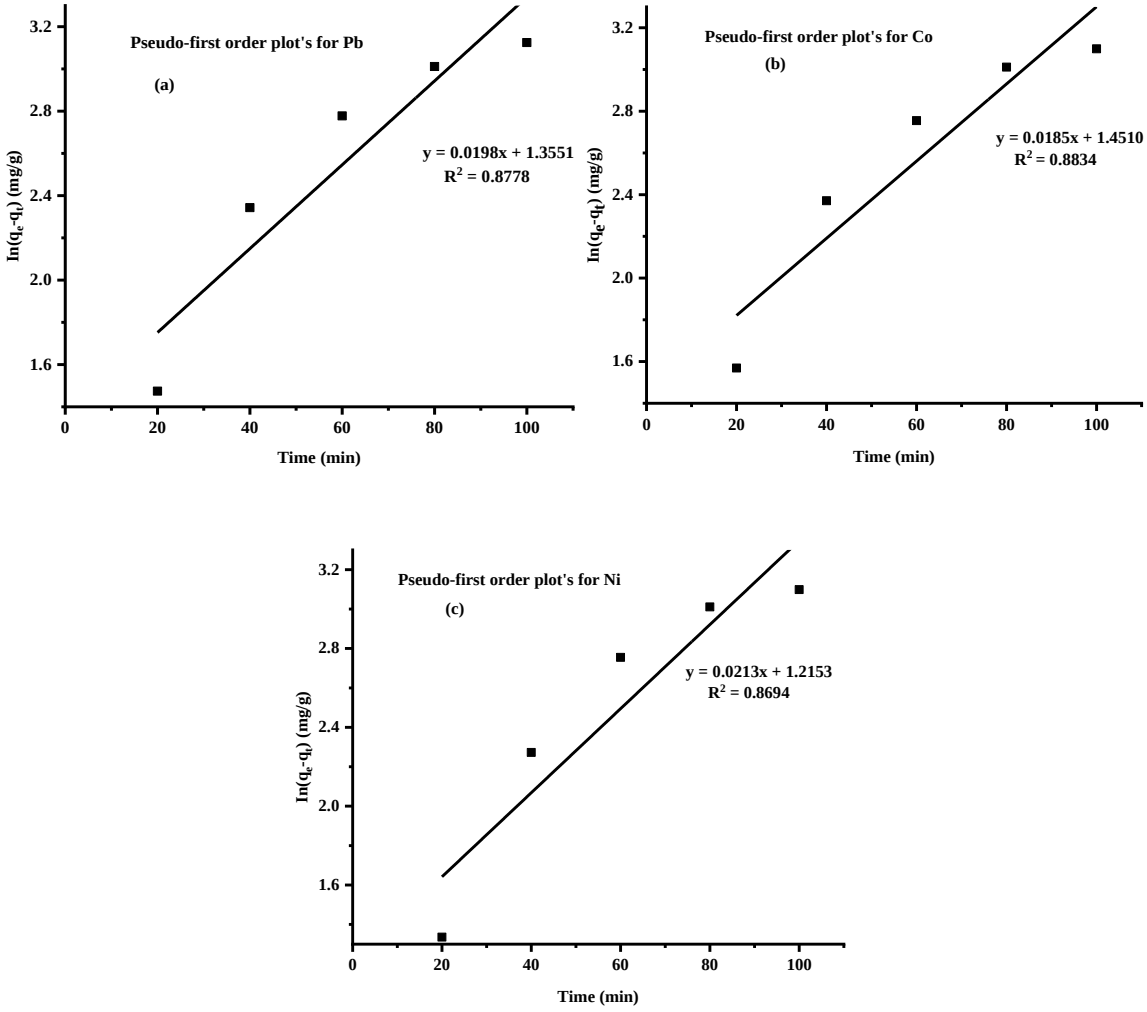

Figure 12. Pseudo-first-order plot for adsorption of (a) Pb^{2+}, (b) Co^{2+}, and (c) Ni^{2+} onto Delonix Regia seed.

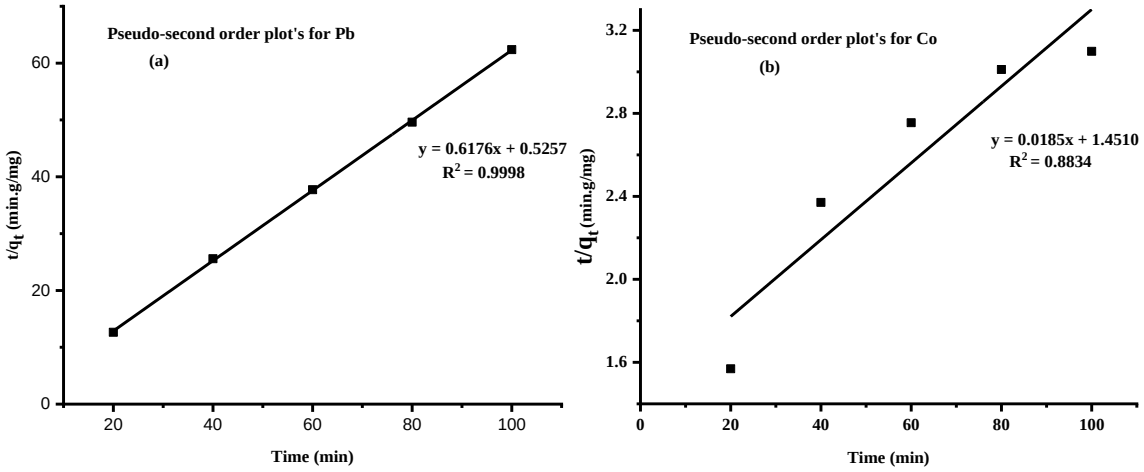

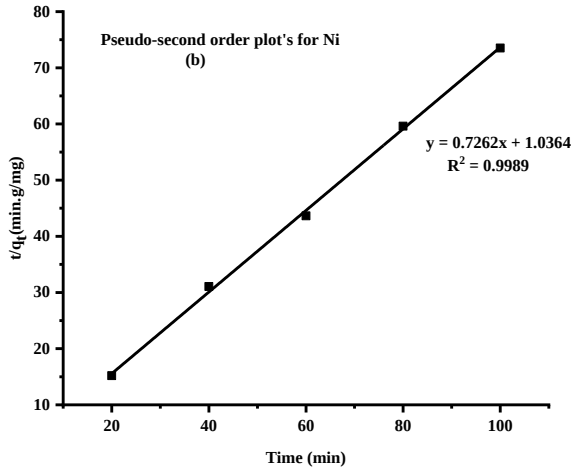

Figure 13. *Pseudo-second-order plot for adsorption of (a) Pb^{2+}, (b) Co^{2+}, and (c) Ni^{2+} onto Delonix Regia seed.*

Table 2. *Parameters for various kinetic models of Pb^{2+}, Co^{2+}, and Ni^{2+} ions onto DRS.*

Kinetic Models	Pb^{2+}	Co^{2+}	Ni^{2+}
Pseudo-first order			
q_e (mg g^{-1})	7.4534	6.7623	6.1267
K_1 (min^{-1})	0.0794	0.06533	0.05947
R^2	0.8778	0.8534	0.8694
Pseudo-second order			
q_e (mg g^{-1})	8.7522	7.6748	7.4562
K_2 (g mg^{-1} min^{-1})	0.0452	0.0551	0.0621
R^2	0.9998	0.8834	0.9989

3.4. Conclusion

The present study demonstrates the potential of *Delonix regia* seed as a low-cost and effective biosorbent for the removal of Pb(II), Ni(II), and Co(II) ions from aqueous solutions. The adsorption performance was influenced by key operational parameters, including solution pH, adsorbent dosage, initial metal-ion concentration, contact time, and temperature. Increasing the adsorbent dosage and contact time generally enhanced metal-ion removal, while the adsorption behaviour was also strongly influenced by solution pH and initial metal-ion concentration.

Equilibrium analysis showed that the Langmuir model provided the best fit for Pb(II) and Co(II) adsorption, with R^2 values of 0.989 and 0.996, respectively. For Ni(II), the Langmuir and Temkin models gave comparable fits, with R^2 values of 0.947 and 0.942, respectively. The Langmuir maximum adsorption capacities were 62.57 mg g^{-1} for Pb(II), 59.26 mg g^{-1} for Co(II), and 73.59 mg g^{-1} for Ni(II), giving the adsorption-capacity order Ni(II) > Pb(II) > Co(II). The favourable Langmuir separation factors obtained for all three metal ions further indicate favourable adsorption under the investigated conditions.

Kinetic analysis showed that the pseudo-second-order model provided a better mathematical description of the adsorption data than the pseudo-first-order model, particularly for Pb(II) and Ni(II). The results indicate that interactions between the dissolved metal ions and the available surface binding sites contribute substantially to the adsorption process. However, the kinetic modelling alone does not provide definitive evidence that chemisorption is the sole or dominant mechanism.

The *Delonix regia* seed shows considerable promise as an inexpensive and sustainable biosorbent for the treatment of metal-contaminated water. Its effective removal performance, simple preparation, and availability make it a potentially useful biomass-based material for wastewater treatment. Further studies should investigate adsorbent regeneration and reuse, adsorption in multicomponent and real wastewater systems, long-term stability, and scale-up to establish its practical applicability.

Abbreviations

DRS	*Delonix Regia* Seed
FTIR	Fourier-transform Infrared Spectroscopy
XRD	X-ray Diffraction
SEM	Scanning Electron Microscopy

Author Contributions

Oyewole Toyib Seun: Conceptualization, Data curation, Formal Analysis, Investigation, Methodology, Writing – original draft, Writing – review & editing

Osundiya Medinat Olubunmi: Resources, Software, Supervision, Validation, Visualization, Writing – original draft

Agumadu Emmanuel Chukwuma: Funding acquisition, Investigation, Methodology, Data curation, Writing – original draft

Ogunbamowo Haminat Temidayo: Data curation, Methodology

Salawu Ismael Eyue: Data curation, Software, Visualization

Idowu Owoyemi Fatai: Data curation, Methodology

Badejo Olayemi Aderanti: Formal Analysis, Investigation

Olowu Rasaq Adewale: Conceptualization, Data curation, Formal Analysis, Writing – review & editing

Conflicts of Interest

The authors declare no conflicts of interest.

References

[1] Abiodun, O.-A. O., Oluwaseun, O., Oladayo, O. K., Abayomi, O., George, A. A., Opatola, E., Orah, R. F., Isukuru, E. J., Ede, I. C., Oluwayomi, O. T., Okolie, J. A., & Omotayo, I. A. (2023). Remediation of heavy metals using biomass-based adsorbents: Adsorption kinetics and isotherm models. *Clean Technologies*, *5*(3), 934-960. https://doi.org/10.3390/cleantechnol5030047

[2] Singh, V., Singh, N., Rai, S. N., Kumar, A., Singh, A. K., Singh, M. P., Sahoo, A., Shekhar, S., Vamanu, E., & Mishra, V. (2023). Heavy Metal Contamination in the Aquatic Ecosystem: Toxicity and Its Remediation Using Eco-Friendly Approaches. *Toxics*, *11*(2), 147. https://doi.org/10.3390/toxics11020147

[3] Sanusi, I. O., Adepoju, A. A., & Abdulrahman, B. D. (2025). Heavy metal contamination, human health impact, and remediation techniques in water bodies: a review. *Discov Environ* 3, 268. https://doi.org/10.1007/s44274-025-00475-5

[4] Nemeș, N. S., Negrea, A., Ciopec, M., Negrea, P., Duțeanu, N., & Duda-Seiman, D. M. (2026). Heavy Metal Ion Removal: A Global Review of Wastewater Treatment Technologies. *International Journal of Molecular Sciences*, *27*(4), 1741. https://doi.org/10.3390/ijms27041741

[5] Zielińska, M., & Bułkowska, K. (2025). Use of Membrane Techniques for Removal and Recovery of Nutrients from Liquid Fraction of Anaerobic Digestate. Membranes, 15(2), 45. https://doi.org/10.3390/membranes15020045

[6] Ayach, J., El Malti, W., Duma, L., Lalevée, J., Al Ajami, M., Hamad, H., & Hijazi, A. (2024). Comparing Conventional and Advanced Approaches for Heavy Metal Removal in Wastewater Treatment: An In-Depth Review Emphasizing Filter-Based Strategies. *Polymers*, *16*(14), 1959. https://doi.org/10.3390/polym16141959

[7] Laishram, D., Kim, S. B., Lee, S. Y., & Park, S. J. (2025). Advancements in Biochar as a Sustainable Adsorbent for Water Pollution Mitigation. *Advanced Science (Weinheim, Baden-Württemberg, Germany)*, *12*(19), e2410383. https://doi.org/10.1002/advs.202410383

[8] Bahsaine, K., Mekhzoum, M. E. M., Benzeid, H., Qaiss, A., & Bouhfid, R. (2022). Recent progress in heavy metals extraction from phosphoric acid: A short review. *Journal of Industrial and Engineering Chemistry*, *115*, 120-134. https://doi.org/10.1016/j.jiec.2022.08.029

[9] Banerjee, J., Bar, N., Basu, R. K., & Das, S. K. (2022). Development of Ni(II)-resistant *Saccharomyces cerevisiae* and its application: Adsorption study and modeling. *Chemosphere*, *309*(Pt 1), 136647. https://doi.org/10.1016/j.chemosphere.2022.136647

[10] Shabir, G., Anwar, F., Sultana, B., Khalid, Z. M., Afzal, M., Khan, Q. M., & Ashrafuzzaman, M. (2011). Antioxidant and antimicrobial attributes and phenolics of different solvent extracts from leaves, flowers, and bark of Gold Mohar [Delonix regia (Bojer ex Hook.) Raf]. *Molecules (Basel, Switzerland)*, *16*(9), 7302–7319. https://doi.org/10.3390/molecules16097302

[11] Essel, V., & Raynie, D. E. (2025). Systematic Isolation and Characterization of Regenerated Hemicellulose and Lignin from Soybean Feedstocks Using Ionic Liquids. *Separations*, *12*(2), 37. https://doi.org/10.3390/separations12020037

[12] Santiago-Martínez, L., Avraamidou, S., Ayala-Cortés, A., Azike, R., Bakshi, S., Banik, C., Bar-Ziv, E., Canales, E., Carlson, T., Dumesic, J. A., Klinger, J. L., Lee, J. M., Long, F., McDonald, A. G., Mohapatra, S., Ong, R. G., Palomo Gonzalez, L. F., Pan, X., Saha, N., Sanchez Castillo, M. A., … Huber, G. W. (2026). Biomass Demineralization: A Critical Need for Future Biorefineries. *Chemical Reviews*, *126*(8), 4511–4591. https://doi.org/10.1021/acs.chemrev.5c00784

[13] Chen, X., Hossain, M. F., Duan, C., Lu, J., Tsang, Y. F., Islam, M. S., & Zhou, Y. (2022). Isotherm models for adsorption of heavy metals from water: A review. *Chemosphere*, *307*(Pt 1), 135545. https://doi.org/10.1016/j.chemosphere.2022.135545

[14] Chen, X., Huang, C., Li, H., Zhao, S., & Zhang, L. (2025). Selective adsorption of vanadyl porphyrin on solid adsorbent in the presence of polycyclic aromatic hydrocarbons. *Chemistry*, *7*(6), 195. https://doi.org/10.3390/chemistry7060195

[15] Edet, U. A., & Ifelebuegu, A. O. (2020). Kinetics, isotherms, and thermodynamic modelling of phosphate adsorption using recycled brick waste. *Processes*, *8*, 665. https://doi.org/10.3390/pr8060665

[16] Eleryan, A., Hassaan, M., Nazir, M. A., Shah, S. S. A., Ragab, S., & El Nemr, A. (2024). Isothermal and kinetic screening of methyl red and methyl orange dye adsorption from water by Delonix regia biochar-sulfur oxide (DRB-SO). *Scientific reports*, *14*(1), 13585. https://doi.org/10.1038/s41598-024-63510-0

[17] El-Sayed, G. O., Dessouki, H. A., & Ibrahiem, S. S. (2011). Removal of Zn(II), Cd(II), and Mn(II) from aqueous solutions by adsorption on maize stalks. *Malaysian Journal of Analytical Sciences*, *15*, 8-21.

[18] Gonçalves, J. O., Leones, A. R., de Farias, B. S., da Silva, M. D., Jaeschke, D. P., Fernandes, S. S., Ribeiro, A. C., Cadaval, T. R. S., Jr., & Pinto, L. A. d. A. (2025). A Comprehensive Review of Agricultural Residue-Derived Bioadsorbents for Emerging Contaminant Removal. *Water*, *17*(14), 2141. https://doi.org/10.3390/w17142141

[19] Hama Aziz, K. H., Mustafa, F. S., Omer, K. M., Hama, S., Hamarawf, R. F., & Rahman, K. O. (2023). Heavy metal pollution in the aquatic environment: efficient and low-cost removal approaches to eliminate their toxicity: a review. *RSC Advances*, *13*(26), 17595-17610. https://doi.org/10.1039/d3ra00723e

[20] He, S. R., Li, Y. T., Weng, L. P., Wang, J. J., He, J. X., Liu, Y. L., Zhang, K., Wu, Q. H., Zhang, Y. L., & Zhang, Z. (2018). Competitive adsorption of Cd^{2+}, Pb^{2+}, and Ni^{2+} onto Fe^{3+}-modified argillaceous limestone. *Science of the Total Environment*, *637-638*, 69-78. https://doi.org/10.1016/j.scitotenv.2018.04.300

[21] Danat, B. T., Wuana, R. A., Chahul, H. F. *et al.* Review of adsorption isotherm models. *Appl Water Sci* 16, 72 (2026). https://doi.org/10.1007/s13201-025-02682-0

[22] Ebada, D., Hefnawy, H. T., Gomaa, A., Alghamdi, A. M., Alharbi, A. A., Almuhayawi, M. S., Alharbi, M. T., Awad, A., Al Jaouni, S. K., Selim, S., Eldeeb, G. S., & Namir, M. (2023). Characterization of *Delonix regia* Flowers' Pigments and Polysaccharides: Evaluating Their Antibacterial, Anticancer, and Antioxidant Activities and Their Application as a Natural Colorant and Sweetener in Beverages. *Molecules (Basel, Switzerland)*, *28*(7), 3243. https://doi.org/10.3390/molecules28073243

[23] Wang, Y., Zhang, Y., Cui, Q., Feng, Y., & Xuan, J. (2024). Composition of Lignocellulose Hydrolysate in Different Biorefinery Strategies: Nutrients and Inhibitors. *Molecules*, *29*(10), 2275. https://doi.org/10.3390/molecules29102275

[24] Silva, T. A. L., Varão, L. H. R., Pasquini, D. (2024). Lignocellulosic Biomass. In: Thomas, S., Hosur, M., Pasquini, D., Jose Chirayil, C. (eds.) Handbook of Biomass. Springer, Singapore. https://doi.org/10.1007/978-981-19-6772-6_5-1

[25] Medinat, O., Abdullahi, S., Oyewole, T. S., Tovide, O. O., Sarah, S., Sewanu, K., & Olowu, R. A. (2024). Adsorption of Pb^{2+} and Mn^{2+} using *Phoenix dactylifera* seed. *Journal of Research and Review in Science*, *11*, 30-46. https://doi.org/10.36108/jrrslasu/4202.11.0192

[26] Shi, Z., Zhu, A., Chen, F., Cai, Y., & Deng, L. (2025). Synthesis of Amorphous MnFe@SBA Composites for Efficient Adsorptive Removal of Pb(II) and Sb(V) from Aqueous Solution. *Molecules*, *30*(3), 679. https://doi.org/10.3390/molecules30030679

[27] Musah, M., Yisa, J., Suleiman, M. A. T., Mann, A., Shaba, E. Y., & Aliyu, A. (2018). Kinetics and isotherm studies of Cr^{6+}, Mn^{2+}, and Cd^{2+} adsorption. *Biological and Environmental Sciences Journal for the Tropics*, *15*(1), 28-34.

[28] Olowu, R. A., Osundiya, M. O., Oyewole, T. S., Onwordi, C. T., Yusuff, O. K., Osifeko, O. L., & Tovide, O. O. (2022). Removal of Zn(II) and Cr(VI) ions using pineapple peels. *European Journal of Applied Sciences*, *10*(5).

[29] Olowu, R. A., Osundiya, M. O., Sobola, A. O., Osifeko, O. L., Tovide, O. O., Oyewole, T. S., Elesho, A. O., Onifade, O. O., Majolagbe, A. O., Onwordi, C. T., & Adejare, A. A. (2024). Sorption of Pb(II), Ni(II), and Cd(II) using tiger nut chaff. *Physical Chemistry*, *13*(2), 19-31. https://doi.org/10.5923/j.pc.20241302.01

[30] Oyewole, T. S., Inuikim, A. E., Osundiya, M. O., Osifeko, O. L., Olowu, R. A. O., Isaac, I. B., Taiwo, R. O., Adejare, A. A., & Oresanya, Z. O. (2023). Equilibrium, Thermodynamics, Kinetics of Adsorption of CO_3^2- and SO_4^2- Ions on Modified Plantain Peels. International Journal of Engineering Research & Science (IJOER), *9*(11), 1-12.

[31] Sui, C., Xie, W., Bian, Y., & Li, X. (2026). Recent Progress in Adsorption Removal of Heavy Metal Ions from Wastewater Using Biomass-Based Materials. *Gels*, *12*(4), 311. https://doi.org/10.3390/gels12040311

[32] Zhu, Q., Ghnim, Z. S., Chandra, S., Makasana, J., Ganesan, S., Shankhyan, A., Kumar, M. R., Sharma, G. C., Adhab, A. H., Mahdi, M. S., Mansoor, A. S., Radi, U. K., Abd, N. S., Herati, K., & Muzammil, K. (2025). Modeling Urotropine adsorption thermodynamics on kaolinite particles. *Scientific reports*, *15*(1), 35143. https://doi.org/10.1038/s41598-025-19112-5

[33] Bakalis, E., & Zerbetto, F. (2025). Adsorption Kinetics: Classical, Fractal, or Fractional?. *Langmuir: the ACS journal of surfaces and colloids*, *41*(30), 19834–19844. https://doi.org/10.1021/acs.langmuir.5c01726

[34] Sandoval-Peraza, V. M., Ramos-Ocharán, O., Alcalá-Escamilla, K. I., Molina-Rosas, M. Y., Chel-Guerrero, L., & Betancur-Ancona, D. (2026). Delonix regia Seed Germ as an Underutilized Biomass Resource: Nutritional Value, Safety, and Potential for Sustainable Protein Supply for Food Systems. *Resources*, *15*(3), 37. https://doi.org/10.3390/resources15030037

[35] Svobodová, E., Tišler, Z., Peroutková, K., Strejcová, K., Abrham, J., Šimek, J., Gholami, Z., & Vakili, M. (2024). Adsorption of Cu(II) and Ni(II) from Aqueous Solutions Using Synthesized Alkali-Activated Foamed Zeolite Adsorbent: Isotherm, Kinetic, and Regeneration Study. *Molecules*, *29*(10), 2357. https://doi.org/10.3390/molecules29102357

[36] Çiçek, A., Sevim, F., Sevim, M., & Kavcı, E. (2025). Adsorption Capacity, Reaction Kinetics and Thermodynamic Studies on Ni(II) Removal with GO@Fe_3O_4@Pluronic-F68 Nanocomposite. *Polymers*, *17*(15), 2141. https://doi.org/10.3390/polym17152141

[37] Nurgain, A., Nazhipkyzy, M., Özsin, G., Zhaparova, A. A., & Apaydın-Varol, E. (2025). Efficient Pb(II) Adsorption by Natural Mugaldzhar Diatomite: Isotherm, Kinetic, and Thermodynamic Analysis. *Journal of Composites Science*, *9*(11), 625. https://doi.org/10.3390/jcs9110625

[38] Bullen, J. C., Saleesongsom, S., Gallagher, K., & Weiss, D. J. (2021). A Revised Pseudo-Second-Order Kinetic Model for Adsorption, Sensitive to Changes in Adsorbate and Adsorbent Concentrations. *Langmuir: the ACS journal of surfaces and colloids*, *37*(10), 3189–3201. https://doi.org/10.1021/acs.langmuir.1c00142

[39] Ye, S., Zhang, W., Hu, X., He, H., Zhang, Y., Li, W., Hu, G., Li, Y., & Deng, X. (2023). Selective Adsorption Behavior and Mechanism for Cd(II) in Aqueous Solution with a Recoverable Magnetic-Surface Ion-Imprinted Polymer. *Polymers*, *15*(11), 2416. https://doi.org/10.3390/polym15112416

[40] Yousef, R., Qiblawey, H., & El-Naas, M. H. (2020). Adsorption as a process for produced water treatment. *Processes, 8*, 1657. https://doi.org/10.3390/pr8121657

[41] Molebatsi, M., Nkoane, B., Keroletswe, N., Chigome, S., & Kabomo, M. T. (2025). The Use of Biosorbents in Water Treatment. Environments, 12(9), 302. https://doi.org/10.3390/environments12090302